



HAL
open science

Blind hyperspectral unmixing using an Extended Linear Mixing Model to address spectral variability

Lucas Drumetz, Simon Henrot, Miguel Angel Veganzones, Jocelyn Chanussot,
Christian Jutten

► **To cite this version:**

Lucas Drumetz, Simon Henrot, Miguel Angel Veganzones, Jocelyn Chanussot, Christian Jutten. Blind hyperspectral unmixing using an Extended Linear Mixing Model to address spectral variability. WHISPERS 2015 - 7th Workshop on Hyperspectral Image and Signal Processing: Evolution in Remote Sensing, Jun 2015, Tokyo, Japan. hal-01165114

HAL Id: hal-01165114

<https://hal.science/hal-01165114>

Submitted on 18 Jun 2015

HAL is a multi-disciplinary open access archive for the deposit and dissemination of scientific research documents, whether they are published or not. The documents may come from teaching and research institutions in France or abroad, or from public or private research centers.

L'archive ouverte pluridisciplinaire **HAL**, est destinée au dépôt et à la diffusion de documents scientifiques de niveau recherche, publiés ou non, émanant des établissements d'enseignement et de recherche français ou étrangers, des laboratoires publics ou privés.

BLIND HYPERSPECTRAL UNMIXING USING AN EXTENDED LINEAR MIXING MODEL TO ADDRESS SPECTRAL VARIABILITY

L. Drumetz¹, S. Henrot¹, M.A. Veganzones³, J. Chanussot^{2,4}, C. Jutten¹

Gipsa-lab, ¹Joseph Fourier University, ²Grenoble Institute of Technology, ³CNRS, Grenoble, France

⁴Faculty of Electrical and Computer Engineering, University of Iceland, Reykjavik, Iceland

ABSTRACT

The Linear Mixing Model is often used to perform Hyperspectral Unmixing because of its simplicity, but it assumes that a single spectral signature can be completely representative of an endmember. However, in many scenarios, this assumption does not hold since many factors such as illumination conditions and intrinsic variability of the endmembers have consequences on the spectral signatures of the materials. In this paper, we propose a simple yet flexible algorithm to unmix hyperspectral data using a recently proposed Extended Linear Mixing Model. This model allows a pixelwise variation of the endmembers, which leads to consider scaled versions of reference endmember spectra. The results on synthetic data show that the proposed technique outperforms other methods aimed at tackling spectral variability, and provides an accurate estimation of endmember variability along the observed scene thanks to the scaling factors estimation, provided the abundance of the corresponding material is sufficient.

Index Terms— Hyperspectral imaging, spectral unmixing, spectral variability, extended linear mixing model

1. INTRODUCTION

Spectral Unmixing (SU) is an inverse problem in hyperspectral remote sensing aimed at recovering the signatures of the materials (endmembers) composing the observed scene, as well as their relative proportions (abundances) in every pixel. In most applications, a Linear Mixing Model (LMM) is assumed, considering that the contributions of each endmember sum up in a linear way [1]. The main two factors hampering the efficiency of the LMM have been identified as nonlinearities and spectral variability. Indeed, many physical processes such as multiple scattering and intimate mixing can contribute to the measured radiance or reflectance spectra in a nonlinear fashion. Spectral variability is also an important factor that the LMM does not take into account: each endmember is implicitly assumed to be perfectly represented by a single spectral signature. This

implicit but strong assumption often does not hold for real datasets since the measured radiance or reflectance of a material can significantly change, e.g. depending on the geometry and topography of the scene, of atmospheric effects or even because of the intrinsic variability of the material, due to the variation of a hidden parameter (e.g. concentration of chlorophyll in vegetation).

Although nonlinear unmixing has recently received much attention in the community, spectral variability has been less addressed in comparison. Still, recent overviews of the spectral variability issue exist and summarize some of the methods that take it into consideration [2, 3]. In the following, we introduce a new algorithm to perform SU taking into account spectral variability. It is based on the recently proposed Extended Linear Mixing Model (ELMM) [4], which can address endmember variability while preserving the LMM framework. The remainder of this paper is organized as follows: Section 2 presents some of the mixing models and techniques related to the proposed approach, which is presented in Section 3. Results are presented in Section 4, and some concluding remarks are gathered in Section 5.

2. RELATED WORK

Let us denote a hyperspectral image by $\mathbf{X} \in \mathbb{R}^{L \times N}$ and the abundance matrix by $\mathbf{A} \in \mathbb{R}^{P \times N}$, where L is the number of spectral bands, N the number of pixels in the image, and P is the number of endmembers. The different endmember matrices we will use will be denoted as $\mathbf{S} \in \mathbb{R}^{L \times P}$, possibly indexed by k if allowed to vary spatially in the image. $\mathbf{E} \in \mathbb{R}^{L \times N}$ is an additive noise. With these notations, the LMM writes, for the pixel $\mathbf{x}_k \in \mathbb{R}^L$, whose abundance vector is $\mathbf{a}_k \in \mathbb{R}^P$:

$$\mathbf{x}_k = \sum_{p=1}^P a_{kp} \mathbf{s}_p + \mathbf{e}_k = \mathbf{S} \mathbf{a}_k + \mathbf{e}_k \quad (1)$$

with the abundance non-negativity constraint (ANC) $a_{kp} \geq 0$ since all the physical quantities involved are positive, and possibly the abundance sum-to-one constraint (ASC) $\sum_{p=1}^P a_{kp} = 1, \forall k$, which means that each pixel has to be completely explained by the contributions of the endmembers. \mathbf{s}_p is the p^{th} column of \mathbf{S} . In the following, some existing approaches

J. Chanussot and C. Jutten are members of Institut Universitaire de France. This work was partially funded by the European Research Council (ERC) under grants ERC AdG-2012-320684 CHESS and ERC AdG-2013-320594 DECODA.

to perform SU by taking into account spectral variability are presented.

2.1. Spectral Bundles

Spectral bundles [5] are a simple way to address endmember variability by building a candidate endmember dictionary. One possibility to do so is to run several times any Endmember Extraction Algorithm (EEA) [1] on randomly chosen subsets of the image. Each time the EEA is run, new instances of each endmember should be extracted. As the extracted sources suffer from the so-called permutation problem, i.e. the endmembers are not aligned from one subset to the other, a clustering step is required to group the candidate endmembers into classes. Then the abundances can be extracted in several ways, e.g. by performing a sparse regression of the data on the dictionary, for instance using the SUNSAL algorithm [6]. To get global abundance maps, one only has to sum the contributions of every candidate in each endmember class. Another option to recover abundances once the spectral bundles have been extracted is to use the Fisher Discriminant Nullspace (FDN) approach [7]. This technique searches for a projection of the dataset onto a low-dimensional subspace such that intra class variability of the endmember bundles is minimized and their interclass variability is maximized. Finally, one can unmix the projected data using the traditional Fully Constrained Least Squares Unmixing (FCLSU), enforcing both the ANC and the ASC (assuming the data lies in a simplex spanned by the sources) using the centroids of the bundles as endmembers.

2.2. Extended Linear Mixing Model

Ideally, the endmembers should be allowed to vary in every pixel of the image, while the mixing process could remain linear. In [4], an Extended Linear Mixing Model (ELMM) is presented to allow a pixelwise variation of each endmember:

$$\mathbf{x}_k = \sum_{p=1}^P a_{kp} f_{kp}(\mathbf{s}_p) + \mathbf{e}_k \quad (2)$$

where f_{kp} are mappings $f_{kp} : \mathbb{R}^L \rightarrow \mathbb{R}^L$. As shown in [4], the spectral bundles approach can also be seen as a special case of (2), where the function f_{kp} is not explicitly but implicitly modeled by some outcomes of this spectral variability function forming the endmember dictionary. If we assume $f_{kp}(\mathbf{s}_p) = \psi_{kp} \mathbf{s}_p$, i.e. that the spectral variability consists in scalings of some reference endmembers collected in the matrix $\mathbf{S}_0 \in \mathbb{R}^{L \times P}$, (2) rewrites:

$$\mathbf{x}_k = \sum_{p=1}^P a_{kp} \psi_{kp} \mathbf{s}_p + \mathbf{e}_k = \mathbf{S}_0 \boldsymbol{\psi}_k \mathbf{a}_k + \mathbf{e}_k \quad (3)$$

with $\boldsymbol{\psi}_i \in \mathbb{R}^{P \times P}$ a diagonal matrix with the ψ_{kp} on the diagonal. With these definitions, an observed pixel is a linear combination of scaled versions of each endmember depending on the spatial dimensions of the image (lying in a convex

cone spanned by the endmembers in \mathbf{S}_0). This special case of the model has appeared implicitly in [8, 9] to explain variability due to the geometry and illumination conditions of the scene. In addition, [4] shows that the nonnegative least squares (CLSU) algorithm can be seen as a special case of equation (3) when the scaling factor is identical for each endmember and the ASC is assumed. Thus, one can recover the scaling factor (and hence the abundances) in a pixel by $\psi_k = \sum_{p=1}^P \hat{\phi}_k^p = \sum_{p=1}^P a_{kp} \psi_k$, where $\hat{\phi}_k^p$ is the quantity estimated by CLSU in pixel k for endmember p . This scaled version of CLSU will be denoted by S-CLSU hereafter. Yet, there is, to our knowledge, no algorithm specifically designed to unmix hyperspectral data according to the model (3).

3. PROPOSED APPROACH

We define the following optimization problem to perform spectral unmixing using the ELMM (we denote by $\boldsymbol{\psi}$ the scaling factors rearranged in a $\mathbb{R}^{P \times N}$ matrix):

$$\mathcal{J}(\mathbf{A}, \underline{\mathbf{S}}, \boldsymbol{\psi}) = \frac{1}{2} \sum_{k=1}^N (\|\mathbf{x}_k - \mathbf{S}_k \mathbf{a}_k\|_F^2 + \lambda_S \|\mathbf{S}_k - \mathbf{S}_0 \boldsymbol{\psi}_k\|_F^2) \quad (4)$$

A reference endmember matrix \mathbf{S}_0 is required, and can be extracted by any EEA. All quantities involved have to be nonnegative, and in addition we enforce the ASC. Since we are estimating the actual abundances and not a product of the abundances and the scaling factors, the ASC is physically meaningful, and also acts as a calibration of the scaling factors (without it, there would be a scaling ambiguity on the abundances and scaling factors: the product of an abundance coefficient in one pixel for one endmember and the corresponding scaling factor is the same if one of the two quantities is multiplied and the other divided by the same constant). Note that compared to eq. (3), a small perturbation on the model is allowed, depending on the value of λ_S . Since the problem we wish to solve is not convex w.r.t. all variables simultaneously, but convex w.r.t. each of them, we propose to find a stationary point by iteratively optimizing the criterion in an Alternating Nonnegative Least Squares (ANLS) way. The iterations terminate when the relative variations (measured using Frobenius norms) between consecutive iterates of \mathbf{A} and $\underline{\mathbf{S}} = \{\mathbf{S}_k\}$ are below ϵ_A and ϵ_S , respectively. In the experiments, we set $\epsilon_A = \epsilon_S = 10^{-4}$.

3.1. Optimization w.r.t. $\underline{\mathbf{S}}$

Rewriting the terms of Eq. (4) depending on $\underline{\mathbf{S}}$, we see that we have to solve:

$$\hat{\underline{\mathbf{S}}} = \arg \min_{\underline{\mathbf{S}} \geq 0} \frac{1}{2} \sum_{k=1}^N (\|\mathbf{x}_k - \mathbf{S}_k \mathbf{a}_k\|_F^2 + \lambda_S \|\mathbf{S}_k - \mathbf{S}_0 \boldsymbol{\psi}_k\|_F^2) \quad (5)$$

This problem is completely separable over the N pixels, so its closed form solution may be computed separately for each of them:

$$\hat{\mathbf{S}}_k \leftarrow (\mathbf{x}_k \mathbf{a}_k^\top + \lambda_S \mathbf{S}_0 \boldsymbol{\psi}_k) (\mathbf{a}_k \mathbf{a}_k^\top + \lambda_S \mathbf{I}_P)^{-1} \quad (6)$$

where \mathbf{I}_P is the $P \times P$ identity matrix. The solution $\hat{\mathbf{S}}_k$ is then projected onto the nonnegative orthant $\mathbb{R}_+^{L \times P}$ by thresholding the negative entries to 0.

3.2. Optimization w.r.t. ψ

Here, the minimization of Eq. (4) w.r.t. ψ rewrites:

$$\hat{\psi} = \arg \min_{\psi \geq 0} \frac{1}{2} \sum_{k=1}^N \lambda_S \|\mathbf{S}_k - \mathbf{S}_0 \psi_k\|_F^2 \quad (7)$$

Recall that for each k , ψ_k is a diagonal matrix, so it is only necessary to update the diagonal coefficients ψ_k^p (the scaling factor associated to the p^{th} endmember of pixel k):

$$\hat{\psi}_k^p \leftarrow \frac{\mathbf{s}_0^{p\top} \mathbf{s}_k^p}{\mathbf{s}_0^{p\top} \mathbf{s}_0^p} \quad (8)$$

where \mathbf{s}_0^p and \mathbf{s}_k^p are the p^{th} columns of the reference endmember matrix and the pixel k endmember matrix, respectively. With this update rule, the coefficients $\hat{\psi}_k^p$ are always nonnegative since all quantities involved in their computations are positive.

3.3. Optimization w.r.t. \mathbf{A}

If we wish to minimize Eq. (4) w.r.t. \mathbf{A} , we have to solve :

$$\hat{\mathbf{A}} = \arg \min_{\mathbf{A} \geq 0, \mathbf{1}_{1 \times P} \mathbf{A} = \mathbf{1}_{1 \times N}} \frac{1}{2} \sum_{k=1}^N \|\mathbf{x}_k - \mathbf{S}_k \mathbf{a}_k\|_F^2 \quad (9)$$

$\mathbf{1}(\cdot)$ is a matrix of ones whose size is given in index. This can be readily solved in each pixel using FCLSU.

4. RESULTS

We generated a simulated $200 \times 200 \times 224$ hyperspectral image incorporating spectral variability using the ELMM. Abundance maps for three endmembers (randomly chosen in a library) consisting in overlapping circular regions was designed. Separately, maps for the spectral variability factors (bounded between 1 and 1.5 in a way such that the reflectance of the sources would never become higher than 1) were generated using mixtures of Gaussians. In order not to be too similar to the ELMM, a small wavelength-dependent nonlinear perturbation (proportional to the square of the reflectance value in the considered band and pixel) was added to every endmember in each pixel (the power ratio between the signal and this this perturbation was set to 50dB). After the mixing process, an additional 30dB white Gaussian noise was added. A RGB representation of the data can be seen in Fig. 1. In the following, we compare the unmixing performance of 6 algorithms (FCLSU, CLSU, S-CLSU, the bundle approach combined with SuNSAL and FDN, and the proposed one), using the abundance overall Root Mean Squared Error (RMSE):

$$RMSE = \frac{1}{N} \sum_{k=1}^N \sqrt{\frac{1}{P} \sum_{p=1}^P (a_{kp} - \hat{a}_{kp})^2} \quad (10)$$

The bundle used was created by running the Vertex Component Analysis (VCA) [9] on 100 randomly chosen subsets comprising 1% of the image pixels. Then the candidate endmembers were clustered using k-means with the spectral angle as a similarity measure (it is insensitive to scalings and hence adapted to the data). The regularization parameter for SuNSAL was set to $5 \cdot 10^{-4}$. As for the proposed approach, two initialization strategies were considered. In the first, the reference endmember matrix was initialized using VCA, the abundances with the results of the FCLSU, and the scaling factors were initially set to one. The Proposed Approach with this initialization is denoted by PA-FCLSU. In the second, the abundances and scaling factors were initialized with the results of S-CLSU (this initialization is denoted by PA-S-CLSU). In both cases, we set an empirically defined value for $\lambda_S = 6.25 \cdot 10^{-1}$. The results are shown in Figs. 2, 3 and in Table 1.

The results show that the proposed approach outperforms all other approaches in terms of abundance estimation. FCLSU gets the worst results since it does not take into account spectral variability. The bundle approaches perform much better, but they are not able to estimate the scaling factors, and erroneous patterns can still be observed in the abundance maps. They also require a balanced and well clustered bundle, which is not always the case depending on the runs. The CLSU approach gets results comparable to the bundle algorithms, but it is not completely accurate because it does not estimate the actual abundances, but their product with the scaling factors. The S-CLSU algorithm performs much better, even though it estimates the same scaling factors for all endmembers. This is in fact not a problem so long as the abundance of one of the materials is high enough. In this case, the estimated scaling factor corresponds to this material. The proposed approach is able to split the scaling factors into individual maps for each material. In the case where the contribution of one endmember is too low, the scaling factor cannot be retrieved, and stays close to one for the proposed approach. Note that it is hard to compare quantitatively the estimated scaling factors to the true ones since the reference endmember matrix is not the same (since for S-CLSU and the proposed approach it was extracted from the image data). From Table 1, we see that the

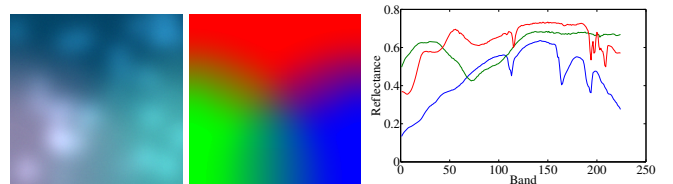


Fig. 1. A RGB representation of the simulated dataset. Note the blob-like shapes corresponding to spectral variability (left). True abundances displayed as a color image (middle). The endmembers used in the experiments (right).

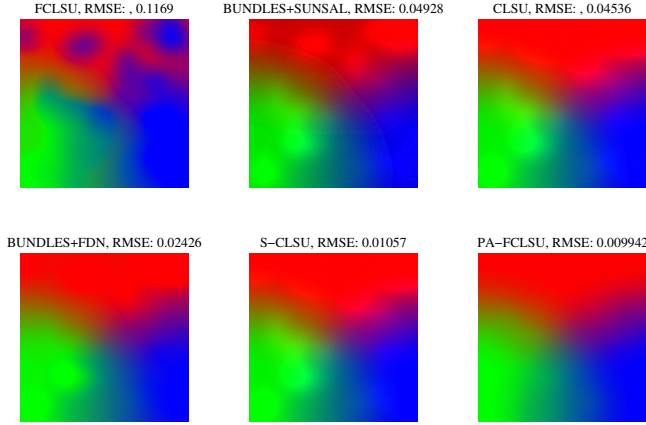


Fig. 2. The estimated abundances of several algorithms.

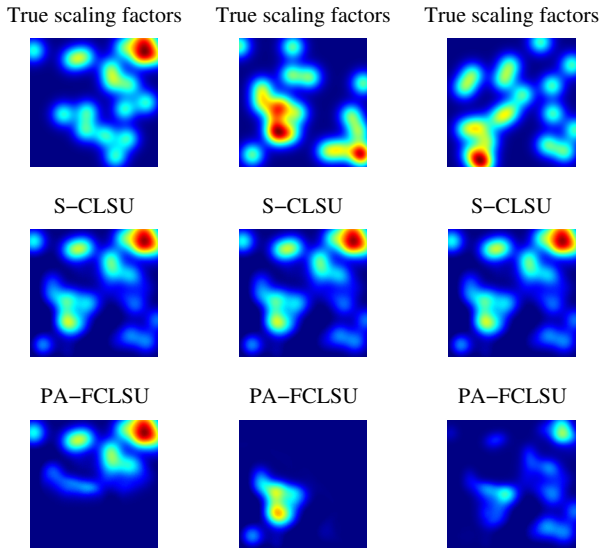


Fig. 3. The estimated scaling factors of S-CLSU and the PA-FCLS. The colormap ranges from blue (1) to red (1.5).

improvement of performance comes at the price of a higher computational burden if the initialization is performed using FCLS and with no guess on the scaling factors. Even when an already very good initialization is provided, the algorithm is still able to improve the results in a short amount of time. However, we believe the proposed approach is more robust than S-CLSU, especially in real scenarios, where nonlinearities, noise and wrong intrinsic dimensionality estimation are likely to happen.

5. CONCLUSION

In this paper, we introduced a simple algorithm to perform hyperspectral image unmixing taking into account spectral variability. The approach is based on the recently proposed Extended Linear Mixing Model, which allows local variations of the endmember matrix using pixel and endmember depen-

Algorithm	Overall RMSE	Running Time (s)
FCLS	0.12	11
BUNDLES + SUNSAT	0.049	14
BUNDLES + FDN	0.024	10
CLSU	0.045	10
S-CLSU	0.011	11
PA-FCLS	0.0099	657
PA-S-CLSU	0.0099	24

Table 1. Quantitative results.

dent scaling factors. The experiments on a synthetic dataset show the potential of the ELM and the flexibility of the proposed approach, which outperforms other methods tackling spectral variability. Nevertheless, the approach still needs to be validated on real datasets. This will be one of the focuses of our future research. We are also currently working on a reference-free formulation of the model, and on improving the algorithm by incorporating a spatial regularization on the estimated scaling factors, so as to obtain spatially more coherent maps and be able to estimate the scaling factors more accurately when pixels are highly mixed.

6. REFERENCES

- [1] J.M. Bioucas-Dias, A. Plaza, N. Dobigeon, M. Parente, Qian Du, P. Gader, and J. Chanussot, "Hyperspectral unmixing overview: Geometrical, statistical, and sparse regression-based approaches," *Sel. Top. in App. Earth Obs. and Rem. Sens., IEEE Journal of*, vol. 5, no. 2, pp. 354–379, April 2012.
- [2] B. Somers, G. P. Asner, L. Tits, and P. Coppin, "Endmember variability in spectral mixture analysis: A review," *Rem. Sens. of Env.*, vol. 115, no. 7, pp. 1603 – 1616, 2011.
- [3] A. Zare and K.C. Ho, "Endmember variability in hyperspectral analysis," *Sig. Proc. Mag., IEEE*, vol. 31, no. 1, pp. 95–104, Jan 2014.
- [4] M.A. Veganzones, L. Drumetz, R. Marrero, G. Tochon, M. Dalla Mura, A. Plaza, J.M. Bioucas-Dias, and J. Chanussot, "A new extended linear mixing model to address spectral variability," in *Proc. IEEE Workshop on Hyp. Image and Sig. Proc.: Evolution in Rem. Sens. (WHISPERS)*, 2014.
- [5] B. Somers, M. Zortea, A. Plaza, and G.P. Asner, "Automated extraction of image-based endmember bundles for improved spectral unmixing," *Sel. Top. in Appl. Earth Obs. and Rem. Sens., IEEE Journal of*, vol. 5, no. 2, pp. 396–408, April 2012.
- [6] J.M. Bioucas-Dias and M.A.T. Figueiredo, "Alternating direction algorithms for constrained sparse regression: Application to hyperspectral unmixing," in *Proc. IEEE Workshop on Hyp. Im. and Sig. Proc.: Evolution in Rem. Sens. (WHISPERS)*, 2010.
- [7] J. Jin, B. Wang, and L. Zhang, "A novel approach based on fisher discriminant null space for decomposition of mixed pixels in hyperspectral imagery," *Geosc. and Rem. Sens. Let., IEEE*, vol. 7, no. 4, pp. 699–703, Oct 2010.
- [8] J.M.P. Nascimento and J.M. Bioucas Dias, "Does independent component analysis play a role in unmixing hyperspectral data?," *Geosc. and Rem. Sens., IEEE Trans. on*, vol. 43, no. 1, pp. 175–187, Jan 2005.
- [9] J.M.P. Nascimento and J.M. Bioucas Dias, "Vertex component analysis: a fast algorithm to unmix hyperspectral data," *Geosc. and Rem. Sens., IEEE Trans. on*, vol. 43, no. 4, pp. 898–910, April 2005.